ISSN 1392-1207. MECHANIKA. Vol. 29, No. 4, 2023: 292–301

Position Decoupling Control of Rigid Rotor of Active Magnetic Bearing

Binglin LI*, Li ZENG**
**Nanjing Forestry University, Nanjing 210037, Jiangsu, China, E-mail: lblqx@njfu.edu.cn*
***Yangzhou University, Yangzhou 225009, Jiangsu, China, E-mail: lzeng@yzu.edu.cn*
https://doi.org/10.5755/j02.mech.31642

1. Introduction

Due to the advantage of no friction, no need of lubrication and long service life, magnetic bearing allows the rotor to run at a high speed. It has a good application prospect in transportation, industry and other fields [1, 2]. Active magnetic bearing can improve rotor stability via the feedback control, however, the five-degree-of-freedom (5-DOF) magnetic bearing has a small coupling effect between the axial and radial directions which can be ignored, so the axial direction can be controlled separately. It should be emphasized that in the radial direction, the four degrees of freedom of magnetic bearing rotor have nonlinear and strong coupling, and it should be considered in the control [3]. For this kind of coupling system, the method adopted by Yang L. et al. is to force decoupling by retaining the diagonal elements of the coupling matrix, and then design decentralized independent controller. The decoupling control method will cause a certain error in the system model, which ignored the gyroscopic effect produced by the high-speed of rotor [4, 5]. Therefore, these control methods are often difficult to meet practical needs. Yi J. et al. adopted the feed-forward decoupling internal model control method to achieve the radial deflection decoupling control [6, 7]. Zheng Shiqiang et al. adopted cross-feedback nutation phase margin tracking compensation control method to achieve nutation modal stability control in the full speed range [8]. All the decoupling methods mentioned above have high requirements on the accuracy of the mathematical model of the control object. When the system control process contains many non-linear and time-varying variables, it is difficult to meet the control requirements. Fang J. et al. used the inverse system solution method to achieve the decoupling of the system, but the method requires the equation to be invertible [9]. The intelligent decoupling method has its advantages in solving system nonlinear problems, such as, neural network systems have self-learning and adaptive capabilities, but it needs to be combined with other control method to satisfy rotor stability control [10]. Moreover, this intelligent decoupling method requires pre-training of samples, which requires a large amount of calculation.

For the control of the magnetic bearing rotor system, the commonly used control methods include LQR control, robust control, adaptive control, etc. [11, 12]. Although the robust control considering the model disturbance has a certain tolerance to the model perturbation, the control method also needs to reasonably choose the sensitivity weighting function [13]. Neural network control requires a lot of training of parameters, which puts forward high requirements for real-time performance and hardware [14]. Liu Yu et al. used the H_∞ method to control the magnetic levitation spindle, However, only the single-degree-of-freedom model of magnetic bearing is analysed, and the position coupling of the rotor is not taken into consideration [15]. Based on the multi-degree-of-freedom magnetic bearing model, Noshadi et al. used the fuzzy PID algorithm to control it，but the inertial coupling problem is also not considered [16]. Among the various control methods mentioned above, some did not consider the coupling problem between the rotor degrees of freedom, or some are forced decoupling of the system, or assumed that there was no inertial coupling in the structure, etc., which would lead to deviations in the control.

What's more, the 5-DOF magnetic bearing is nonlinear and its parameters are difficult to accurately estimate and predict, thereupon, it is necessary to adopt a robust control method for the 5-DOF magnetic bearing rotor system. Sliding mode control has the advantages of fast response, insensitive to parameter changes, and easy control to achieve [1]. It can achieve parameter uncertainty or time-varying systems control; therefore, it is used in this paper.

This paper proposes a linear output feedback method for decoupling the active magnetic bearing system and designs a controller based on sliding mode control for controlling a 5-DOF magnetic bearing. The controller assures the control stability and robustness to the variations in the system parameters and disturbances due to the external disturbance of the magnetic bearing. According to the dynamic characteristics of the magnetic bearing, the 5-DOF mathematical model of the magnetic bearing control system is developed; the coupling problem between the degrees of freedom is analyzed; and the linear output feedback method is applied to decouple the system. Finally, the sliding mode controller is designed, and the control performance of other controllers after decoupling the system is compared.

The organization of the paper is as follows: a magnetic bearing dynamic model is presented in section a II; and linear output feedback is used to decouple the magnetic bearing model in section III; Fuzzy PD controller and Sliding mode variable structure controller are designed in section IV. Two representative simulation results are discussed in section V. The last section concludes this paper.

2. AMB-Rotor system dynamic model

2.1. Radial active magnetic bearing model

The basic principle of the active magnetic bearing control system in one degree of freedom is shown in Fig. 1. Active magnetic bearings generate electromagnetic force *f*, by applying current to make the rotor levitate to the desired position. In a typical stable active magnetic bearing model, the rotor is levitated at its equilibrium point (i_0, x_0), x_0 is

at the center of two magnets and i_0 is the corresponding bias current of winding. As is usual in AMB systems, the radial electromagnetic bearing is driven in a differential mode. One electromagnet is driven by the sum of the bias current and control current i_0+i_j, the other one is driven by their difference i_0-i_j. Once the rotor deviates from the equilibrium position x_0 by disturbance, the distance between the rotor and the desired position is detected by the position sensor, and then the controller obtains the information and outputs proper voltages to the power amplifiers, which in turn apply currents to the electromagnets. The electromagnets then generate magnetic forces to balance the rotor to the desired position.

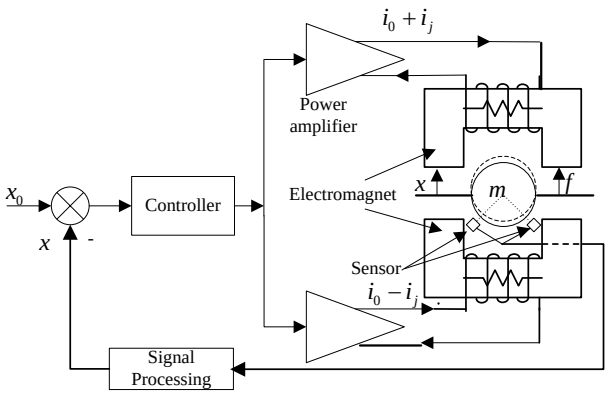

Fig. 1 Working principal diagram of active magnetic bearing system

It is assumed that the leakage magnetic flux, eddy current loss, and edge effect of the magnetic flux are not considered. The electromagnetic force generated by the active magnetic bearing in radial direction can be expressed as:

$$f=\mu_0 S_0\left(\frac{ni}{2x}\right)^2=\frac{1}{4}\mu_0 n^2 S_0\frac{i^2}{x^2}=K\frac{i^2}{x^2}, \tag{1}$$

where: $K=\frac{1}{4}\mu_0 n^2 S_0$; μ_0 is the vacuum permeability; n is the number of the coil turns on the magnetic actuator; S_0 is the cross-sectional area of magnetic pole; x is the rotor position detected by the sensor. It can be seen from Eq. (1) that as the current i of the electromagnetic actuators increases, the electromagnetic force obtained by the rotor increases; as the gap x between the rotor and the electromagnet increases, the electromagnetic force obtained by the rotor decreases.

For the U-shaped magnetic pole structure in Fig. 1, the force f represents the difference of forces between both magnets, which affect the rotor with an angle α. Considering the effect, there is:

$$f=K\frac{i^2}{x^2}\cos\alpha. \tag{2}$$

Since the AMB system is driven in a differential mode, one magnet is driven by current i_0+i_j, the other one driven by the difference i_0-i_j, as shown in Fig. 1, so the electromagnetic coil can generate positive and negative forces on the rotor. In Eq. (2), i is replaced by i_0+i_j and i_0-i_j, similarly, the air gap x is replaced by x_0-x_j and x_0+x_j,so the electromagnetic force can be expressed as:

$$F_j=K\cos\alpha\left[\left(\frac{i_0-i_j}{x_0-x_j}\right)^2-\left(\frac{i_0+i_j}{x_0+x_j}\right)^2\right], \tag{3}$$

where: i_j, x_j are the control current and rotor displacement at the j-th degree of freedom, respectively, and x_0 is the given air gaps. It can be seen from the Eq. (3) that the electromagnetic force of each degree of freedom is squared with the ratio of the current to the air gap. The force of the two counteracting magnets at an operating point can be deduced into the linear form by Taylor series expansion:

$$F_j=K_{xj}x_j+K_{ij}i_j\quad j=1,\cdots,5, \tag{4}$$

where: $K_{ij}=\frac{\mu_0 n^2 S_0 i_0^2}{x_0^2}\cos\alpha$ and $K_{xj}=\frac{\mu_0 n^2 S_0 i_0}{x_0^3}\cos\alpha$,which are called current force stiffness coefficient and displacement force stiffness coefficient on the j-th degree of freedom, respectively.

2.2. Rotor system model

The force of the magnetic bearing rotor is shown in Fig. 2, the rigid rotor is suspended by two radial magnetic bearings and one axial magnetic bearing. The position sensor and the magnetic actuator coil are integrated on a plane, which simplifies the position coupling of the sensor. As mentioned above, the axial and radial degrees of freedom of rigid rotor systems have only small couplings; axial motion is considered as a single degree of freedom in the magnetic bearing-rotor system. So, the axial and radial motions of the rotor can be analysed and controlled separately.

It is assumed that the electromagnetic force uniformly distributed on the rotor is a concentrated force, and its direction is consistent with the central axis of the rotor, and there is no resultant moment.

Since the gravity of the rotor is much smaller than the electromagnetic force, the influence of the rotor's gravity is ignored [13]. It is assumed that the rotor is rigid and symmetric, that is, the moments of inertia on the x, y axis are equal.

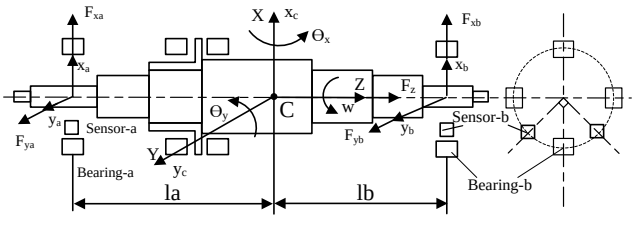

Fig. 2 Structure and force analysis of magnetic suspension rotor

The parameter values of magnetic levitation are shown in Table 1 [17].

Table 1

System variables and parameter values

Parameters	Symbol	Value
Mass of rotor, kg	*m*	2.8
Rotary of inertia of axis *X*, kg/m^2	*Jx*	0.0214
Rotary of inertia of axis *Y*, kg/m^2	*Jy*	0.0214
Rotary of inertia of axis *Z*, kg/m^2	*Jz*	7.646×10^{-4}
Distance from "a" to mass center, m	*la*	0.1217
Distance from "b" to mass center, m	*lb*	0.13383
Radial displacement stiffness, N/m	*Kxr*	-3.2368×10^5
Axial displacement stiffness, N/m	*Kxz*	-6.2359×10^6
Radial current stiffness, N/A	*Kir*	43.7931
Axial current stiffness, N/A	*Kiz*	748.3099

According to Newton's second law, dynamic equations of the rotor can be expressed as follows:

$$\begin{cases} m\cdot\ddot{x}_c = F_{xa} + F_{xb} \\ m\cdot\ddot{y}_c = F_{ya} + F_{yb} \\ m\cdot\ddot{z}_c = F_{zc} \\ J_x\cdot\ddot{\theta}_x = F_{ya}\cdot l_a - F_{yb}\cdot l_b - J_z\cdot\omega\cdot\dot{\theta}_y \\ J_y\cdot\ddot{\theta}_y = -F_{xa}\cdot l_a + F_{xb}\cdot l_b + J_z\cdot\omega\cdot\dot{\theta}_x \end{cases}, \tag{5}$$

where: m is the rotor mass; J_x and J_y are the rotary of inertia of X, Y axis, and J_z is the rotary of inertia of Z axis; F_{uv} represents the force of the rotor at the supporting point of v and the direction of the axis u, ($v = a, b$; $u = x, y$); F_{zc} is the force of the rotor in the Z-axis direction; x_c, y_c and z_c are the displacement of the rotor in the X-axis, Y-axis, and Z-axis directions at the center of mass, respectively; θ_x and θ_y are the rotation angles of the rotor around the X-axis and Y-axis at the center of mass, respectively; l_a and l_b are the distances between the position sensors and the center of mass; ω is the rotor speed.

Since the sensor position is in the plane a, b, the displacement parameters that can be obtained are x_a, x_b, y_a and y_b respectively. So, x_c, y_c and θ_x, θ_y can be replaced by x_a, x_b, y_a and y_b, and Eq. (6) can be expressed according to the geometric relationship:

$$\begin{cases} x_c = (l_b\cdot x_a + l_a\cdot x_b)/l \\ y_c = (l_b\cdot y_a + l_a\cdot y_b)/l \\ \theta_x = (y_a - y_b)/l \\ \theta_y = (-x_a + x_b)/l \\ l = l_a + l_b \end{cases}. \tag{6}$$

According to Eq. (4), the electromagnetic force F_{xa}, F_{xb}, F_{ya}, F_{yb}, F_z can be expressed as:

$$\begin{cases} F_{xa} = K_{xr}\cdot x_a + K_{ir}\cdot i_{xa} \\ F_{xb} = K_{xr}\cdot x_b + K_{ir}\cdot i_{xb} \\ F_{ya} = K_{xr}\cdot y_a + K_{ir}\cdot i_{ya} \\ F_{yb} = K_{xr}\cdot y_b + K_{ir}\cdot i_{yb} \\ F_z = K_{xz}\cdot z_c + K_{iz}\cdot i_{zc} \end{cases}. \tag{7}$$

Describe Eq. (5) in the form of a state space equation as:

$$\begin{aligned} \dot{X} &= AX + BU \\ Y &= CX + DU \end{aligned}, \tag{8}$$

where: state vector $X = [x_a, x_{b,} y_a, y_b, z_c, \dot{x}_a, \dot{x}_{b,} \dot{y}_a, \dot{y}_b, \dot{z}_c]$, control vector $U = [i_{xa}, i_{xb,} i_{ya}, i_{yb}, i_{zc}]^T$, output vector $Y_s = [x_a, x_{b,} y_a, y_b, z_c]^T$, $A = \begin{bmatrix} O_{5\times5} & I_{5\times5} \\ a_{21} & a_{22} \end{bmatrix}$,

$C_s = \begin{bmatrix} I_{5\times5} & O_{5\times5} \end{bmatrix}_{5\times10}$, $B = \begin{bmatrix} O_{5\times5} \\ b_{22} \end{bmatrix}_{10\times5}$, $D = O_{5\times5}$,

$$a_{21} = \begin{bmatrix} \frac{K_{xr}}{m} + \frac{l_a^2 K_{xr}}{J_y} & \frac{K_{xr}}{m} - \frac{l_a l_b K_{xr}}{J_y} & 0 & 0 & 0 \\ \frac{K_{xr}}{m} - \frac{l_a l_b K_{xr}}{J_y} & \frac{K_{xr}}{m} + \frac{l_b^2 K_{xr}}{J_y} & 0 & 0 & 0 \\ 0 & 0 & \frac{K_{xr}}{m} + \frac{l_a^2 K_{xr}}{J_x} & \frac{K_{xr}}{m} - \frac{l_a l_b K_{xr}}{J_x} & 0 \\ 0 & 0 & \frac{K_{xr}}{m} - \frac{l_a l_b K_{xr}}{J_x} & \frac{K_{xr}}{m} + \frac{l_b^2 K_{xr}}{J_x} & 0 \\ 0 & 0 & 0 & 0 & \frac{K_{xz}}{m} \end{bmatrix},$$

$$a_{22} = \begin{bmatrix} 0 & 0 & -\frac{l_a J_z \omega}{l J_y} & \frac{l_a J_z \omega}{l J_y} & 0 \\ 0 & 0 & \frac{l_a J_z \omega}{l J_y} & -\frac{l_a J_z \omega}{l J_y} & 0 \\ \frac{l_a J_z \omega}{l J_x} & -\frac{l_a J_z \omega}{l J_x} & 0 & 0 & 0 \\ -\frac{l_b J_z \omega}{l J_x} & -\frac{l_b J_z \omega}{l J_x} & 0 & 0 & 0 \\ 0 & 0 & 0 & 0 & 0 \end{bmatrix},$$

$$b_{21} = \begin{bmatrix} \frac{K_{ir}}{m} + \frac{l_a^2 K_{ir}}{J_y} & \frac{K_{ir}}{m} - \frac{l_a l_b K_{ir}}{J_y} & 0 & 0 & 0 \\ \frac{K_{ir}}{m} - \frac{l_a l_b K_{ir}}{J_y} & \frac{K_{ir}}{m} + \frac{l_b^2 K_{ir}}{J_y} & 0 & 0 & 0 \\ 0 & 0 & \frac{K_{ir}}{m} + \frac{l_a^2 K_{ir}}{J_x} & \frac{K_{ir}}{m} - \frac{l_a l_b K_{ir}}{J_x} & 0 \\ 0 & 0 & \frac{K_{ir}}{m} - \frac{l_a l_b K_{ir}}{J_x} & \frac{K_{ir}}{m} + \frac{l_b^2 K_{ir}}{J_x} & 0 \\ 0 & 0 & 0 & 0 & \frac{K_{iz}}{m} \end{bmatrix}.$$

3. Linear output feedback decoupling of magnetic bearing rotor

The state space Eq. (8) can be expressed in another form of differential Eq. (9). It can be seen that, except for the degrees of freedom in the Z-axis direction, the equations form in the remaining four degrees of freedom

are basically the similar. From the analysis of coupling relationship, x_a and x_b exist not only in the differential term of the second derivative of x_a, but also in the second differential term of x_b, which is also called inertial coupling.

$$\begin{cases} \ddot{x}_a = \left(\frac{K_{xr}}{m} + \frac{l_a^2 K_{xr}}{J_y}\right) x_a + \left(\frac{K_{xr}}{m} - \frac{l_a l_b K_{xr}}{J_y}\right) x_b + \left(\frac{K_{ir}}{m} + \frac{l_a^2 K_{ir}}{J_y}\right) i_{xa} + \left(\frac{K_{ir}}{m} - \frac{l_a l_b K_{ir}}{J_y}\right) i_{xb} - \frac{l_a J_z \omega}{l J_y}(\dot{y}_a - \dot{y}_b) \\ \ddot{x}_b = \left(\frac{K_{xr}}{m} - \frac{l_a l_b K_{xr}}{J_y}\right) x_a + \left(\frac{K_{xr}}{m} + \frac{l_b^2 K_{xr}}{J_y}\right) x_b + \left(\frac{K_{ir}}{m} - \frac{l_a l_b K_{ir}}{J_y}\right) i_{xa} + \left(\frac{K_{ir}}{m} + \frac{l_b^2 K_{ir}}{J_y}\right) i_{xb} + \frac{l_b J_z \omega}{l J_y}(\dot{y}_a - \dot{y}_b) \\ \ddot{y}_a = \left(\frac{K_{xr}}{m} + \frac{l_a^2 K_{xr}}{J_x}\right) y_a + \left(\frac{K_{xr}}{m} - \frac{l_a l_b K_{xr}}{J_x}\right) y_b + \left(\frac{K_{ir}}{m} + \frac{l_a^2 K_{ir}}{J_x}\right) i_{ya} + \left(\frac{K_{ir}}{m} - \frac{l_a l_b K_{ir}}{J_x}\right) i_{yb} + \frac{l_a J_z \omega}{l J_x}(\dot{x}_a - \dot{x}_b) \\ \ddot{y}_b = \left(\frac{K_{xr}}{m} - \frac{l_a l_b K_{xr}}{J_x}\right) y_a + \left(\frac{K_{xr}}{m} + \frac{l_b^2 K_{xr}}{J_x}\right) y_b + \left(\frac{K_{ir}}{m} - \frac{l_a l_b K_{ir}}{J_x}\right) i_{ya} + \left(\frac{K_{ir}}{m} + \frac{l_b^2 K_{ir}}{J_x}\right) i_{yb} - \frac{l_b J_z \omega}{l J_y}(\dot{x}_a - \dot{x}_b) \\ \ddot{z}_c = \left(\frac{K_{xz}}{m}\right) z_c + \left(\frac{K_{iz}}{m}\right) i_{zc} \end{cases} \tag{9}$$

Therefore, there is a coupling relationship between x_a and x_b, which is related to the structure of the rotor itself. The coupling relationship between y_a and y_b is similar. In addition to the inertial coupling relationship between the degrees of freedom on the *x*, *y* axis, there is also a gyroscopic effect coupling between the radial four degrees of freedom of the axis because of the coefficient term ω contained on the axis *x*, *y* which is related to the rotor speed. According to related research [14], when the rotational speed of the rotor is below 60000 r/min, compared with inertial coupling, the gyroscopic coupling has little influence on the system and can be ignored.

Assuming that the rotor rotational speed is lower than 60000r/min in the paper, so the gyroscopic coupling between the axis *x*, *y* of the system can be ignored. Therefore, there is only inertial coupling between the two degrees of freedom in *x*, *y* direction of rotor. Only by decoupling it can it be regarded as independent system and then it can be controlled independently. Since the Z-axis system is relatively independent, it can be controlled separately. Then the paper only focuses on the decoupling control of the *x*, *y* axis. In the following, a coupling system composed of two degrees of freedom on the *x*-axis is taken as an example for study, and the solution for the *y* -axis is similar. The *x*-degree-of-freedom system is a two-input two-output system, and the system model is described as follows:

$$\begin{aligned} \dot{X}_s &= A_s X_s + B_s U_s \\ Y_s &= C_s X_s \end{aligned}, \tag{10}$$

where: state vector $X_s = [x_a, x_b, \dot{x}_a, \dot{x}_b]^T$, control vector $U_s = [i_{xa}, i_{xb}]^T$, output vector $Y_s = [x_a, x_b]^T$, the parameter matrix $A_s = \begin{bmatrix} O_{2\times 2} & I_{2\times 2} \\ \frac{K_{xr}}{m} + \frac{l_a^2 K_{xr}}{J_y} & \frac{K_{xr}}{m} - \frac{l_a l_b K_{xr}}{J_y} \quad 0 \quad 0 \\ \frac{K_{xr}}{m} - \frac{l_a l_b K_{xr}}{J_y} & \frac{K_{xr}}{m} + \frac{l_b^2 K_{xr}}{J_y} \quad 0 \quad 0 \end{bmatrix}$,

$$B_s = \begin{bmatrix} O_{2\times 2} \\ \frac{K_{ir}}{m} + \frac{l_a^2 K_{ir}}{J_y} & \frac{K_{ir}}{m} - \frac{l_a l_b K_{ir}}{J_y} \\ \frac{K_{ir}}{m} - \frac{l_a l_b K_{ir}}{J_y} & \frac{K_{ir}}{m} + \frac{l_b^2 K_{ir}}{J_y} \end{bmatrix}, \quad C_s = [I_{2\times 2} \quad O_{2\times 2}].$$

As long as Eq. (10) is decoupled, the system will become two independent subsystems. In general, the state space equation of a system can be decoupled under certain conditions by selecting an appropriate feedback matrix. For the system involved in this article, the system output is the displacement of the rotor, which can be directly measured by the position sensor. In this way, the output variable can be measured, which greatly facilitates the design of the controller, so the output feedback decoupling is adopted. The principle of linear output feedback decoupling is shown in Fig. 3.

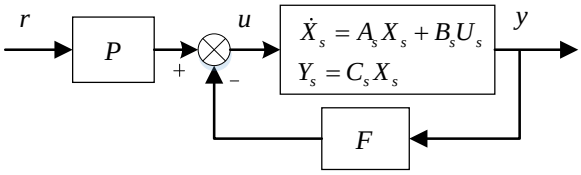

Fig. 3 Linear output feedback decoupling principle

From Fig. 3, the output feedback law is:

$$u = -F \cdot y + P \cdot r, \tag{11}$$

where: F is the feedback matrix; P is the compensation matrix. So, the corresponding closed-loop state equation is:

$$\dot{X}_s = (A_s - B_s F C_s) X_s + B_s P \cdot r. \tag{12}$$

Linear output feedback decoupling is the required constant decoupling matrix pair (F, P), making the $H(s)$ matrix a diagonally rational matrix.

$$H(s) = C_s (sI - A_s + B_s F C_s)^{-1} B_s P. \tag{13}$$

If a suitable matrix F, P can be obtained by adopting a certain method, the closed-loop transfer function matrix $H(s)$ can be made into a non-singular diagonal matrix, that is, 2 independent subsystems, so as to achieve the decoupling between the various degrees of freedom of rotor.

Output feedback decoupling can be obtained by generalizing the state feedback decoupling, so the design of the state feedback decoupling can be performed firstly. According to the well-known Morgan's theorem, the existence of a linear output feedback matrix pair (K, P) makes the closed-loop system decoupling condition is as follow $\det(B_s^*) \neq 0$. B_s^* is called the decoupling matrix, which plays an important role in decoupling calculations. It is defined as $B_s^* = \begin{bmatrix} c_1^T A_s^{d1} B_s \\ c_2^T A_s^{d2} B_s \\ \cdots \\ c_m^T A_s^{dm} B_s \end{bmatrix}$, where c_i^T is the i-th row of matrix C_s; d_i is called the decoupling index, which is an important indicator of the state of each subsystem. It is defined as follows:

$$d_i = \begin{cases} min\{k \mid c_i^T A_s^k B_s \neq 0, k = 0,1,2\cdots n-1\} \\ n-1, \text{for all } k, \text{there is } c_i^T A_s^k B_s = 0 \end{cases}. \quad (14)$$

If $\det(B_s^*) \neq 0$, , it is a system without inherent coupling. Then the closed-loop system can be decoupled by state feedback.

Substitute the system parameters into Eq. (14) and calculate as $d_1 = 1$, $d_2 = 1$ and $B_s^* = \begin{bmatrix} 48.91860 & -18.6947 \\ -18.6947 & 56.043 \end{bmatrix}$.

It can be seen that $\det(B_s^*) \neq 0$, therefore, there exists a linear output feedback matrix pair (K, P) to achieve the decoupling of the system. The matrix K, P can be obtained by the following equation:

$$\begin{cases} K = \left(B_s^*\right)^{-1} \left(C_s * + \sum_{k=0}^{\delta} M_k C_s A_s^k\right) \\ P = \left(B_s^*\right)^{-1} \Gamma_0 \end{cases}, \quad (15)$$

where: $\delta = max\{d_i\}$, $M_k = diag\{m_{k1}, m_{k2}, \cdots, m_{km}\}$, Γ_0 can choose any diagonal matrix, in order to simplify the calculation, let it be a unit matrix. The coefficient of the diagonal matrix M_k determines the pole configuration of the closed-loop system. To reduce the amount of calculation, M_0 and M_1 are all taken as zero matrices, that is, all poles are configured as zero poles.

Substituting the relevant data to calculate, the matrices K and P obtained respectively are

$$P = \begin{bmatrix} 0.0234 & 0.0077 \\ 0.0077 & 0.0202 \end{bmatrix}, \; K = \begin{bmatrix} 7.9994e3 & -0.0107 & 0 & 0 \\ -0.0689 & 7.9996e3 & 0 & 0 \end{bmatrix}.$$

Linear output feedback is a generalized form of linear state feedback, according to Eq. (11) $u = -K \cdot x + P \cdot r = -FC_s x + P \cdot r = -F \cdot y + P \cdot r$. So:

$$K = FC_s, \quad (16)$$

where: r is the 2-dimensional vector of the desired input.

For $\text{rank}\begin{bmatrix} K \\ C_s \end{bmatrix} = \text{rank}[C_s] = 2$.

Therefore, the matrix F exists, and the system can be decoupled by linear output feedback. From Eq. (16), the value of the feedback matrix F can be obtained as $F = \begin{bmatrix} 7.9994e3 & -0.0107 \\ -0.0689 & 7.9996e3 \end{bmatrix}$.

According to the system state equation given by Eq. (10) and the calculated matrix F and P values, the closed-loop transfer function of the system can be calculated as:

$$H(s) = C_s(sI - A_s + B_s F C_s)^{-1} B_s P = diag\{1/s^2, 1/s^2\}. \quad (17)$$

According to the Eq. (17), the decoupled system includes two uncoupled second-order integral subsystems, which can be controlled separately.

4. Design of controller of magnetic bearing

According to the decoupled magnetic levitation model established in the previous section, a controller needs to be designed to make it levitate stably. Meanwhile, a fuzzy PD controller will be designed to compare the control performance with the SMC controller.

4.1. Design of fuzzy PD controller

Fuzzy controller has good robustness performance. Firstly, fuzzy PD controller is used to control the decoupled system, and the principle is shown in Fig. 4. The input variable of the fuzzy inference module is the deviation e and its differentiation de/dt. The output variables Δkp and Δkd are used to correct the PD controller coefficient in real time. After many trials, the initial values of kp and kd are chose as 150 and 20 respectively. The domains of e and de/dt are [-2.5e-5, 2.5e-5] and [-5e-5, 5e-5] respectively. Divide the two domains of e and de/dt into seven equal parts: [-2.5e-5, -1.66e-5, -0.833e-5, 0, 0.833e-5, 1.66e-5, 2.5e-5] and [-5e-5, -3.33 e-5, -1.66e-5, 0, 1.66e-5, 3.33e5, 5e-5], corresponding to fuzzy logic sets are {NB, NM, NS, ZO, PS, PM, PB}. The output domains of Δkp and Δkd are [-30, +30], [-20, +20] respectively. The membership functions of input and output variables are shown in Figs. 5 and 6 respectively.

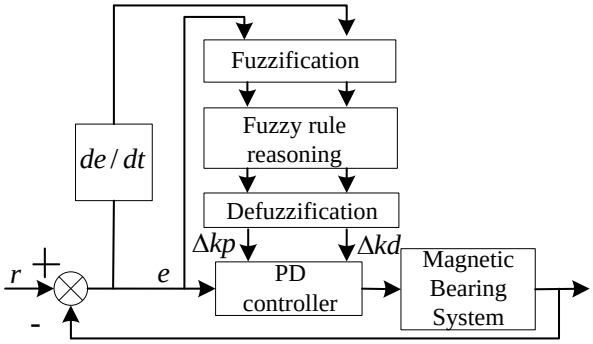

Fig. 4 Fuzzy PD controller principle

Based on the consideration of system stability, response speed, overshoot and other factors, it is necessary to establish appropriate control parameters and their self-tuning rules. In this method, when e is larger, the value of Δkp should be increased to speed up the system response. In order not to saturate the system differential due to the sudden increase of e in the early stage of the response, so that the control effect is not within the allowable range, the value of Δkd should be reduced. When the magnitudes of e and de/dt are relatively moderate, in order to reduce the overshoot of the system response, the value of Δkp should be appropriately reduced; when e is small, the value of Δkd should be appropriately increased, which can make the steady-state performance of the system better. When de/dt is larger, Δkp should take a smaller value.

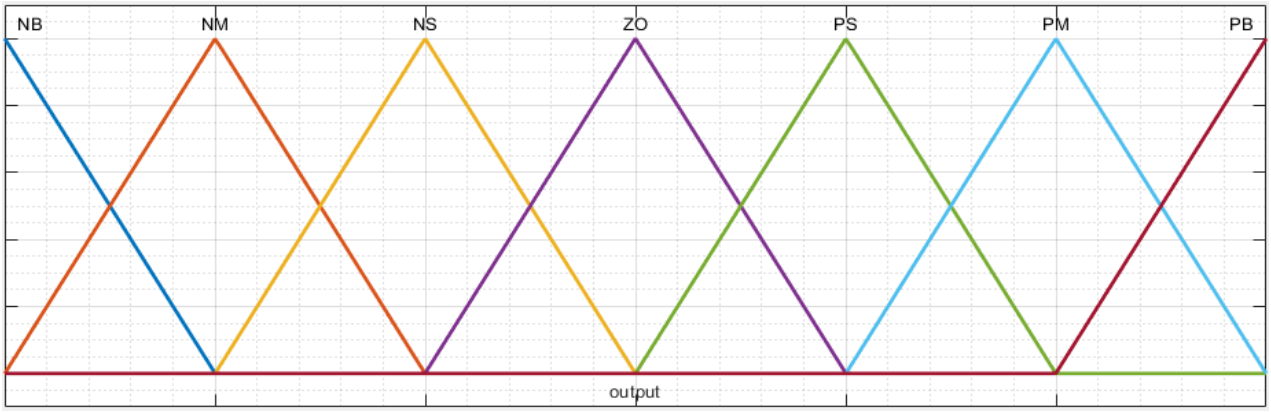

Fig. 5 Input membership function

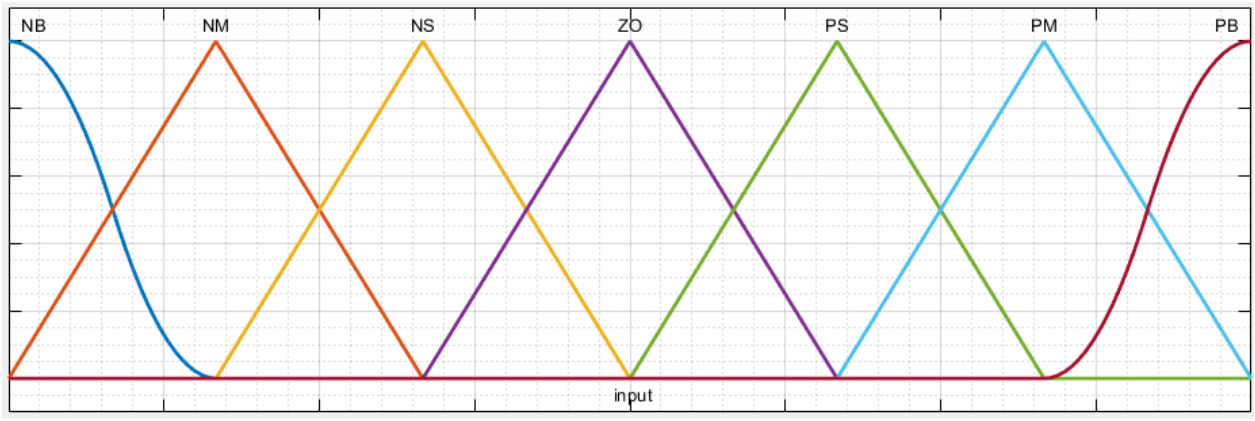

Fig. 6 Output membership function

According to the above-mentioned parameter adjustment rules and the previous experience in the control of magnetic levitation systems, and combined with the movement law of the suspended rotor to analyze and summarize, the fuzzy control rules of the system are established as shown in Table 2.

Table 2

Fuzzy control rule table

kp/*kd*		*de*/*dt*						
		NB	NM	NS	ZO	PS	PM	PB
e	NB	PB/NS	PB/NS	PB/NS	PB/NS	PB/NS	PB/NS	PB/NS
	NM	PS/PS	PS/PS	PS/PS	PS/PS	PS/PS	PS/PS	PS/PS
	NS	PS/PB	PS/PB	PS/PB	PS/PB	PS/PS	PS/PS	PS/PB
	ZO	ZO/PB	ZO/PB	ZO/PB	ZO/PB	ZO/PB	ZO/PB	ZO/PB
	PS	PS/PB	PS/PS	PS/PS	PS/PB	PS/PB	PS/PB	PS/PB
	PM	PS/PS	PS/PS	PS/PS	PS/PS	PS/PS	PS/PS	PS/PS
	PB	PB/NS	PB/NS	PB/NS	PB/NS	PB/NS	PB/NS	PB/NS

4.2. Design of sliding mode variable structure controller

In the AMB controller, sliding mode control is proposed because of the nonlinear characteristics of the system and the high demand of controller in accuracy, robustness and responsiveness. Although the method will cause system chattering, it can be effectively reduced by different reaching law functions [15]. Equation (10) can be written as a multiple-input multiple-output system, which can be expressed as:

$$\begin{cases} \begin{bmatrix} \dot{x}_1(t) \\ \dot{x}_2(t) \end{bmatrix} = \begin{bmatrix} A_{11} & A_{12} \\ A_{21} & A_{22} \end{bmatrix} \begin{bmatrix} x_1(t) \\ x_2(t) \end{bmatrix} + \begin{bmatrix} 0 \\ B_{21} \end{bmatrix} u(t) \\ y(t) = [C_{11} \ C_{12}] \begin{bmatrix} x_1(t) \\ x_2(t) \end{bmatrix} \end{cases}, \tag{18}$$

where: $x_1 \in R^{n-p}$, $x_2 \in R^p$, $u \in R^p$.

Assuming r is a desired input, the error is described as:

$$\delta = r - x_1(t). \tag{19}$$

Then the error rate of change can be described as:

$$\dot{\delta} = \dot{r} - x_2(t). \tag{20}$$

Supposed $V = [v, 1]$, the error vector is

$E=[\delta \ \dot{\delta}]^T$, the sliding mode surface function is designed as follows:

$$s = VE = v[r - x_1(t)] + \dot{r} - x_2(t). \tag{21}$$

So, its differential equation can be written as:

$$\dot{s} = v[\dot{r} - \dot{x}_1(t)] + \ddot{r} - \dot{x}_2(t). \tag{22}$$

Combined with Eq. (15), its differential form is further expressed as:

$$\dot{s} = v[\dot{r} - x_2(t)] + \ddot{r} - A_{21}x_1(t) - A_{22}x_2(t) - B_{21}u, \tag{23}$$

where: v satisfies the Hurwitz polynomial.

Sliding mode variable structure control will produce high-frequency chattering for the system. The exponential approach law can shorten the approach time, make the system variable movement reach the switching surface at a very low speed, and weaken the system chattering. The law of exponential approach is defined as:

$$\dot{s} = -\varepsilon sgn(s) - ks, \tag{24}$$

where: $\varepsilon > 0$, $k > 0$ are chose parameters. From Eq. (18), the sliding mode control law is defined as:

$$u = B_{21}^{-1}\{v[\dot{r} - x_2(t)] + \ddot{r} - A_{21}x_1(t) - \\ -A_{22}x_2(t) - \varepsilon sgn(s) - ks\}. \tag{25}$$

The tracking error of the system composed of the decoupled system model and the designed controller must be bounded and stable. According to the chose sliding mode switching surface, the Lyapunov function is chosen as:

$$V = s^2 / 2. \tag{26}$$

There force, its differential equation can be written as:

$$\dot{V} = s\dot{s} = s(v\dot{\delta} + \ddot{\delta}) = \\ = s[-ks - \varepsilon \,\mathrm{sgn}(s)] = -ks^2 - \varepsilon|s|, \tag{27}$$

where: k, ε, v are constants more than zero. It can be calculated that $\dot{V} < 0$ from the Eq. (27). Under the sliding mode control of exponential reaching law, the tracking error of the system is bounded and stable.

According to the magnetic bearing decoupling model discussed above, the matrix coefficients of Eq. (10) can be obtained and are expressed as $A_{11} = \begin{bmatrix} 0 & 0 \\ 0 & 0 \end{bmatrix}$, $A_{12} = \\ = \begin{bmatrix} 1 & 0 \\ 0 & 1 \end{bmatrix}$, $A_{21} = \begin{bmatrix} 0 & 0 \\ 0 & 0 \end{bmatrix}$, $A_{22} = \begin{bmatrix} 0 & 0 \\ 0 & 0 \end{bmatrix}$, $B_{21} = \begin{bmatrix} 1 & 0 \\ 0 & 1 \end{bmatrix}$, $C_{11} = \\ = \begin{bmatrix} 1 & 0 \\ 0 & 1 \end{bmatrix}$, $C_{12} = \begin{bmatrix} 1 & 0 \\ 0 & 1 \end{bmatrix}$.

The final sliding mode control law can be obtained by substituting these parameters into Eq. (25).

5. Results and discussions

Computer simulations are performed to verify the effectiveness of the decoupling control method designed by Matlab/Simulink for the 5-DOF magnetic bearing. The desired position of control is to make the rotor stably levitate at 0.125 mm from the geometric center of the magnetic bearing and compare the control performance of PD controller, fuzzy PD controller and sliding mode variable structure controller (SMC).

5.1. Position response control

The input signal is a step signal, which is used to simulate the step response performance of the suspended rotor under different controllers. Three cases of conventional PD controller, Fuzzy PD controller (with the same initial parameters) and sliding mode controller (SMC) control applied to the magnetic bearing are simulated respectively. The simulation results are shown in Fig. 7. In Figure, the blue solid lines represent the case SMC controller; the red dashed-lines represent the case with Fuzzy PD controller, the violet dashed-dotted lines represent the case with PD controller.

It can be known that in the case of ordinary PD controller, with control parameter kp=150, kd =20, the adjustment time of is 0.497 s and no overshoot. By comparing the control performance of ordinary PD controller, it can also be known that in the case of Fuzzy PD control, with the same initial parameters, the adjustment time is obviously shortened to 0.277s, but there is a little overshoot. It needs to be emphasized that in the case of sliding mode controller, with control parameters v =100, ε =0.001 the adjustment time is 0.05 s, which has faster response performance than the two controllers mentioned above.

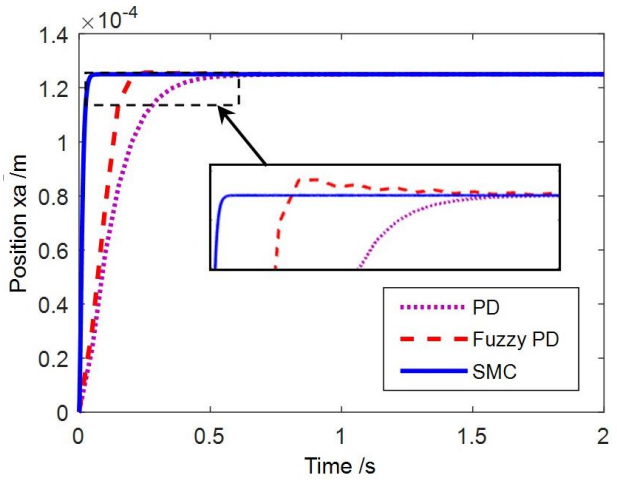

Fig. 7 Comparison of position response of three control methods

Fig. 8 shows the control performance comparison between the decoupling and non-decoupling of the magnetic levitation with four degrees of freedom at x_a=0.125 mm, x_b=y_a=y_b=0 mm. It can be seen from the simulation results that due to the coupling characteristics between variables, although the un-decoupled magnetic suspension system is

controlled by PID, x_a, x_b, y_a and y_b all oscillate, which cannot be controlled at the desired position, and the control performance is difficult to meet the requirements. However, after the system is decoupled and controlled, it stabilizes at 0.125mm after a certain oscillation and overshoot, and the other three x_b, y_a and y_b have been stabilized at the given desired position of 0mm, indicating that the system has been successfully decoupled in the coordinate X and Y directions, and achieved good results.

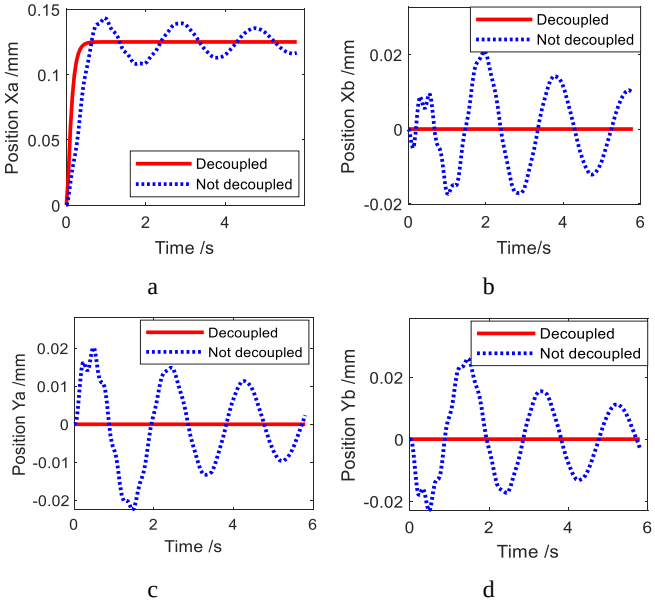

Fig. 8 Position response of the system with 4-DOF

5.2. Anti-disturbance control

In order to know the anti-disturbance performance of the system after decoupling, the control desired values of x_a, x_b, y_a and y_b are all set to 0.125 mm, and then external disturbance is added in the displacement direction of x_a at 1 s to make it deviate from the equilibrium position by 0.2 mm.

Three cases of conventional PD controller, Fuzzy PD controller (with the same initial parameters) and sliding mode controller (SMC) control also applied to the magnetic bearing are simulated respectively. The simulation results are shown in Fig. 9. In figure, the violet solid lines represent the case SMC controller; the blue dashed-dotted represent the case with Fuzzy PD controller, the red dashed-lines lines represent the case with PD controller.

By comparing the control performance of different methods, it can also be known that in the case of SMC controller, with control parameters v=100, ε=0.001, under the influence of external disturbance, the displacement change of x_a is much smaller than that of conventional PD controller and Fuzzy PD controller. In detail, PD controller and fuzzy PD controller are almost equivalent in anti-disturbance performance, resulting in an excessive overshoot. Although it finally stabilized at the desired position, it deviates too much from it during the adjustment process. However, when the SMC controller is used, under the influence of external disturbance, the displacement change is very small, and it is almost always maintained at the desired position, indicating that SMC has a good anti- disturbance performance.

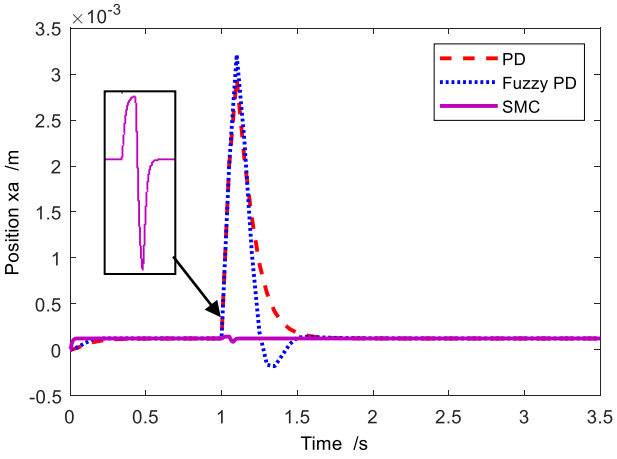

Fig. 9 Comparison of anti-disturbance output of three control methods

In order to observe the control stability of the four degrees of freedom in the radial direction of the rotor under SMC controller when the rotor is subjected to external disturbances, it can be known from Fig. 10 that there are fluctuations in the x_a direction. After being controlled by SMC, it can still remain stable, as shown in Fig. 10a. The remaining three degrees of freedom x_b, y_a and y_b are always stable at the desired position, as shown in Fig. 10b–d, which shows that the degrees of freedom are independent of each other and prove the successful decoupling of the system. Therefore, SMC controller can make the system resist the influence brought by disturbance and has strong anti- disturbance performance.

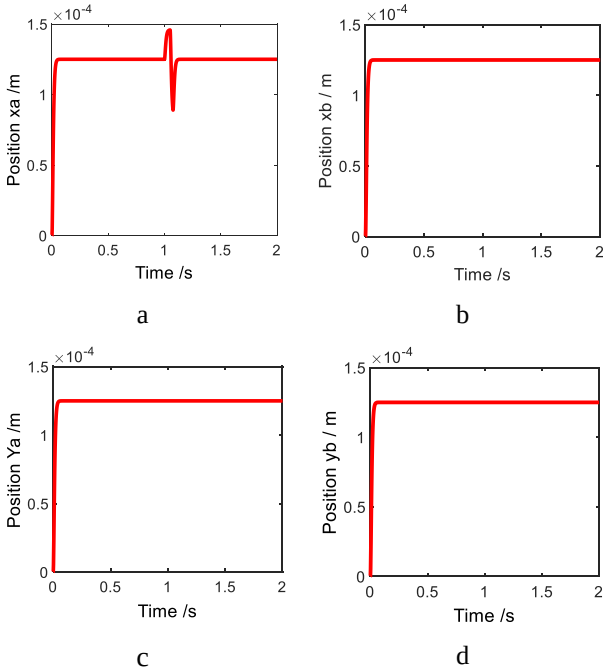

Fig. 10 The output of each degree when disturbance is applied in the x_a direction

5.3. Tracking control

In order to enable the suspension rotor to track the required suspension height requirements, a reference tracking signal with an amplitude of 0.14 ± 0.3mm and a frequency of 10 rad/s is given in the x_b direction, and the desired value of other degrees of freedom is given as 0.125

mm to verify the tracking of the SMC controller algorithm performance.

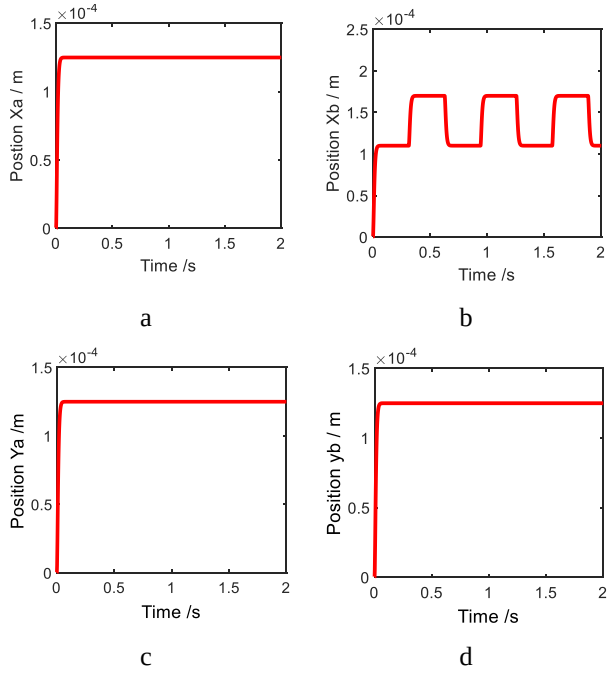

Fig. 11 The output of each degree when a square wave is input in the x_b direction

It can be known from Fig. 11 that the control results can track the desired value on each degree of x_a, x_b, y_a and y_b, indicating that the SMC controller can make the rotor track desired position.

Through the comparative analysis of the control results of position response, it is concluded that the PD controller, fuzzy PD controller and SMC controller can ensure the stability of the system without overshooting. However, compared with the difference in control performance, SMC controller has very good rapidity and response characteristics than the first two controllers. Moreover, SMC controller makes the controlled system have better anti-disturbance performance, so that the rotor reaches a stable state more quickly and smoothly. Finally, the controller can achieve the rotor to quickly track the desired position.

6. Conclusions

A 5-DOF magnetic bearing model was established and the radial coupling problem of the magnetic bearing rotor was analyzed. The study looked into the control problem of AMB coupling relationship, and proposed a control method applied to the stability control based on sliding mode control. In the decoupling method, the rotor system is decoupled through linear output feedback decoupling, which achieves the independence of the four degrees of freedom in the radial direction of the magnetic suspension rotor. In the process of control, the sliding mode controller is designed. The dynamic performance and stability characteristic of the AMB with the proposed SMC controller are better than the conventional PD controller and fuzzy PD controller. Moreover, the SMC controller can effectively improve the performance of the AMB in term of anti-disturbance and signal tracking performance, so it has the advantage of robustness. This paper only studies the decoupling control of active magnetic bearing from the simulation, and the experimental verification research should be studied in the future.

Acknowledgements

The work was supported by National Natural Science Foundation of China (Grant Nos. 51375427), Natural Science Foundation of the Jiangsu Higher Education Institutions (Grant No. 13KJB580006).

References

1. **Lee, H.; Kim, K.; Lee, T.** 2006. Review of maglev train technologies, IEEE Transactions on Magnetics 42(7): 1917-1925. http://dx.doi.org/10.1109/TMAG.2006.875842.
2. **Pichot, M. A.; Kajs, J. P.; Murphy, B. R.;** et al. 2001. Active magnetic bearings for energy storage systems for combat vehicles, IEEE Transactions on Magnetics 37(1): 318-323. http://dx.doi.org/10.1109/20.911846.
3. **Hutterer, M.; Hofer, M.; Schrdl, M.** 2015. Decoupled control of an active magnetic bearing system for a high gyroscopic rotor, IEEE International Conference on Mechatronics: 210-215. http://dx.doi.org/ 10.1109/ICMECH.2015.7083976.
4. **Yang, L.; Shuaishuai, M.; Siyao, Z.;** et al. 2019. Research on automatic balance control of active magnetic bearing-rigid rotor system, Shock and Vibration 2019: 1-14. http://dx.doi.org/ 10.1155/2019/3094215.
5. **Guan, X.; Zhou, J.; Jin, C.;** et al. 2020. Disturbance suppression in active magnetic bearings with adaptive control and extended state observer, Proceedings of the Institution of Mechanical Engineers Part I Journal of Systems and Control Engineering 234(2): 272-284. http://dx.doi.org/ 10.1177/0959651819849774.
6. **Yi, J.; Ren, G. P.; Zhang, H. T. ;** et al. 2019. A model reference adaptive controller with feedforward decoupling for active magnetic bearing rotor system, 2019 IEEE 4th Advanced Information Technology, Electronic and Automation Control Conference (IAEAC), IEEE 12: 833-838. http://dx.doi.org/ 10.1109/IAEAC47372.2019.8998078.
7. **Zhao, H. Y. ; Zhu, C. S.** 2019. Feedforward decoupling control for rigid rotor system of active magnetically suspended high-speed motors, IET Electric Power Applications 13(9): 1298-1309. http://dx.doi.org/ 10.1049/iet-epa.2018.5824.
8. **Zheng, S. ; Feng, R.** 2016. Feedforward compensation control of rotor imbalance for high-speed magnetically suspended centrifugal compressors using a novel adaptive notch filter, Journal of Sound and Vibration 366: 1-14. http://dx.doi.org/ 10.1016/j.jsv.2015.12.029.
9. **Fang, J.; Ren, Y.** 2012. Decoupling control of magnetically suspended rotor system in control moment gyros based on an inverse system method, IEEE/ASME Transactions on Mechatronics 17(6): 1133-1144.
10. **Sun, Y. ; Xu, J. ; Qiang, H. ;** et al. 2019. Adaptive sliding mode control of maglev system based on RBF neural network minimum parameter learning method, Measurement 141: 217-226.

http://dx.doi.org/ 10.1109/TMECH.2011.2159618.
11. **Dong, L.; You, S.** 2014. Adaptive control of an active magnetic bearing with external disturbance, Isa Transactions 53(5): 1410-1419. http://dx.doi.org/ 10.1016/j.isatra.2013.12.028.
12. **Kandil, M. S.; Dubois, M. R.; Bakay, L. S.;** et al. 2017. Application of second-order sliding mode concepts to active magnetic bearings, IEEE Transactions on Industrial Electronics PP(99): 1-10. http://dx.doi.org/ 10.1109/TIE.2017.2721879.
13. **Kuseyri, İ. S.** 2012. Robust control and unbalance compensation of rotor/active magnetic bearing systems, Journal of Vibration & Control 18(6): 817-832. http://dx.doi.org/ 10.1177/1077546310397560.
14. **Avdesh Singh Pundir**; **Kailash Singh**. 2019. Chattering free sliding mode control with observer based adaptive radial basis function neural network for temperature tracking in a fixed bed reactor, International Journal of Chemical Reactor Engineering, 17(10): 20180256. https://doi.org/10.1515/ijcre-2018-0256.
15. **Kang, H.; Oh, S. Y.; Song, O**. 2011. H-infinity control of a rotor-magnetic bearing system based on linear matrix inequalities, Journal of Vibration and Control (2): 291-300. http://dx.doi.org/ 10.1177/1077546310362449.
16. **Noshadi, A.; Shi, J.; Lee, W. S.;** et al. 2016. Optimal PID-type fuzzy logic controller for a multi-input multi-output active magnetic bearing system, Neural Comput & Applic 27: 2031–2046. http://dx.doi.org/10.1007/s00521-015-1996-7.
17. **Li, B. L.; Zeng, L.; Zhang, P. M.;** et al. Sliding mode active disturbance rejection decoupling control for active magnetic bearings, Electric Machines and Control 025(007): 129-138 (in Chinese). http://dx.doi.org/ 10.15938/j.emc.2021.07.014.

B. Li, L. Zeng

POSITION DECOUPLING CONTROL OF RIGID ROTOR OF ACTIVE MAGNETIC BEARING

S u m m a r y

The magnetic bearing rotor system has the problem of positional coupling in the direction of the radial degrees of freedom. This paper proposes a linear output feedback method which decouples the multi-variable coupling system into four single-degree-of-freedom second-order integral subsystems. Firstly, a five-degree-of-freedom (5-DOF) mathematical model of active magnetic bearing rotor is derived. Then, a sliding mode variable structure controller is designed for the decoupled subsystems and the stability of system is guaranteed by the Lyapunov stability theory. The results of computer simulation show that the design controller of sliding mode variable structure controller can more effectively enhance the magnetic bearing rotor performance stability compared with the conventional PD controller, fuzzy PD controller, no matter in the position respond control and anti-disturbance control. Moreover, the sliding mode variable structure controller make the system have better tracking performance.

Keywords: magnetic bearings; position control; decoupling; linear output feedback method; sliding mode control.

Received January 18, 2022
Accepted August 2, 2023